Chem Biol Drug Des 2011; **77:** 399–411

Review

doi: 10.1111/j.1747-0285.2011.01110.x

Insight into Amyloid Structure Using Chemical Probes

Ashley A. Reinke and Jason E. Gestwicki*

Department of Biological Chemistry, Pathology and the Life Sciences Institute, University of Michigan, Ann Arbor, MI 48109-2216, USA
**Corresponding author: Jason E. Gestwicki, gestwick@umich.edu*

Alzheimer's disease (AD) is a common neurodegenerative disorder characterized by the deposition of amyloids in the brain. One prominent form of amyloid is composed of repeating units of the amyloid-β (Aβ) peptide. Over the past decade, it has become clear that these Aβ amyloids are not homogeneous; rather, they are composed of a series of structures varying in their overall size and shape and the number of Aβ peptides they contain. Recent theories suggest that these different amyloid conformations may play distinct roles in disease, although their relative contributions are still being discovered. Here, we review how chemical probes, such as Congo red, thioflavin T and their derivatives, have been powerful tools for the better understanding of amyloid structure and function. Moreover, we discuss how design and deployment of conformationally selective probes might be used to test emerging models of AD.

Key words: Alzheimer's disease, amyloid beta, Congo red, curcumin, fibrils, oligomers, protofibrils, thioflavin T

Abbreviations: AD, Alzheimer's disease; AFM, atomic force microscopy; APP, amyloid precursor protein; Aβ, amyloid-β; CG, Chrysamine G; CR, Congo red; FRET, Forster resonance energy transfer; FTIR, Fourier transform infrared; HCR, hydrophobic core region; HDX, hydrogen-deuterium exchange; LMW, low molecular weight; LTP, long-term potentiation; MD, molecular dynamics; SAR, structure–activity relationship; TEM, transmission electron microscopy; ThT, thioflavin T.

Amyloid-β (Aβ) is a short (38–42 residue) fragment of the amyloid precursor protein. Under physiological conditions, Aβ peptides adopt a β-sheet-type secondary structure that is prone to self-assembly into higher-order structures, including dimers, trimers, oligomers, protofibrils, and the fibrils that are characteristic of patients with late-stage Alzheimer's disease (AD). These conformations are defined by their signature appearances by electron and atomic force microscopy, their size on polyacrylamide gels, and even their method of preparation (Figure 1). Collectively, these aggregates are severely neurotoxic (1,2) and some of them also appear to inhibit long-term potentiation and promote synaptic loss (3–5). The most recent, emerging variants of the Amyloid Hypothesis propose that the prefibrillar amyloids, such as oligomers and other soluble structures (Abeta-derived diffusable ligands (ADDLs), protofibrils, etc.), might play a particularly central role in disease (6–9). However, despite advances in our understanding of Aβ biochemistry and AD pathology, the mechanisms of neurodegeneration are still not clear. One challenge is that amyloids, especially prefibrillar structures, are structurally heterogeneous and conformationally dynamic, which has complicated routine structural studies. Although progress has certainly been made using advanced methods, such as solid-phase nuclear magnetic resonance (NMR) and computational simulations (10–13), many important questions remain. What molecular features do amyloids share? How do different amyloid conformers vary in their topology? What are the mechanisms of neurodegeneration and which specific features of amyloids contribute to toxicity? These are clearly pressing questions, as more than 35 million people suffer from AD and this afflicted population is expected to grow rapidly without a clear disease-modifying therapeutic available.

Small molecules that bind to amyloids, such as the widely used thioflavin T (ThT) and Congo red (CR), have been essential tools in the study of Aβ aggregation. In part, the strength of these compounds is their versatility; they have been used to monitor self-assembly *in vitro*, to recognize Aβ deposits *in vivo* and to identify aggregation inhibitors. In addition, these compounds have been used to probe the structure of various amyloids, and these studies have provided insights into the molecular features of the binding sites. Here, we review what is known about the binding of small molecules to amyloids and summarize what these studies have revealed about the relationships between amyloid structure and function.

Thioflavin T

Binding to aggregated Aβ enhances ThT fluorescence

Thioflavin T is a benzothiazole-based dye (Figure 2A) first noted to bind amyloid by Vassar and Culling in 1959 (14) and later used in studying patient-derived amyloids by Naiki *et al.* (15–17). These groups noted that the fluorescence of ThT is quenched in solution, but that its quantum yield is greatly increased when bound to the β-sheet structure of amyloid fibrils (18). This same phenomenon was observed with synthetic Aβ fibrils (19), and ThT was adapted by LeVine (20) into a convenient, inexpensive assay for monitoring fibril formation *in vitro*. This protocol has been largely unchanged and is perhaps the most widely employed method for monitoring Aβ aggregation.

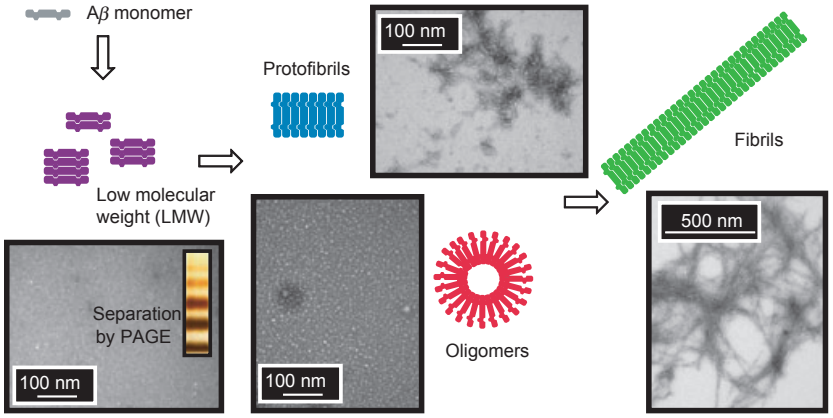

Figure 1: Amyloid-β self-assembles into a variety of distinct conformations. Monomers assemble into dimers, trimers, and other low-molecular-weight oligomers, which proceed to form larger oligomers and protofibrils. Mature fibrils have a characteristic, elongated morphology. Electron micrographs of enriched samples are shown.

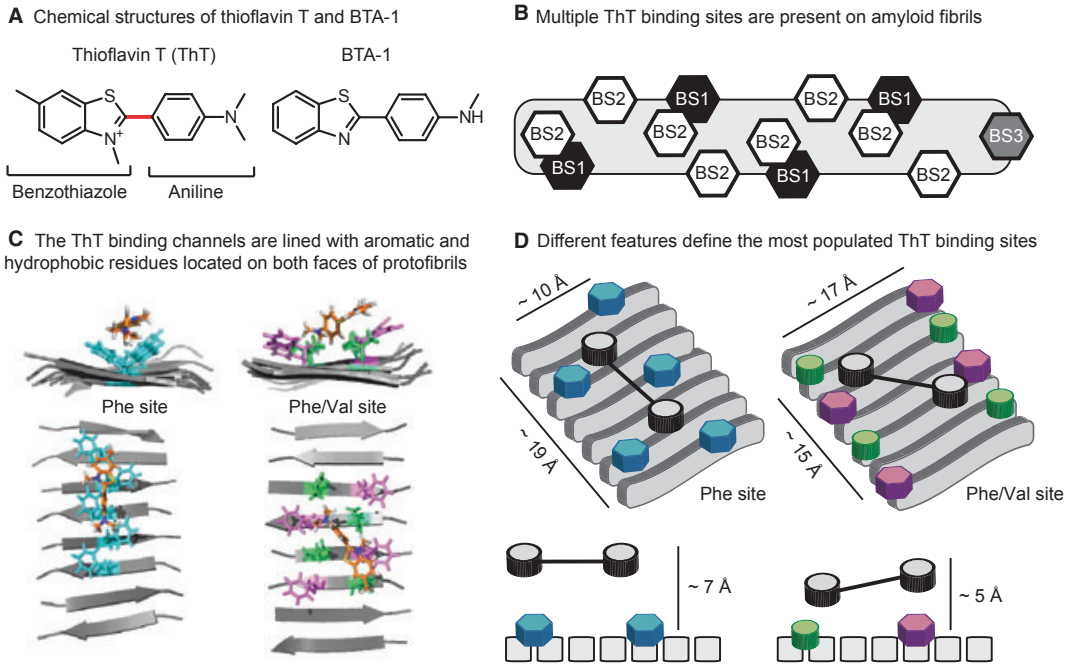

Figure 2: Thioflavin T (ThT) binds amyloids at multiple sites. (A) Chemical structures of ThT and a neutral analog, BTA-1, highlighting the major components: a benzothiazole ring system attached to functionalized aniline. The linker between these modules is shown in red. (B) Amyloids contain three distinct ThT binding sites, two with high density (BS1 and BS2) and one with low density (BS3). (C) Snapshots from molecular dynamics simulations illustrate ThT binding within two channels lined with either Phe residues (left) or both Phe and Val residues (right) (27,28). (D) A schematic model of the two ThT binding sites, illustrating their unique molecular features. The same color scheme is used in parts C and D.

Thioflavin T fluorescence is thought to increase when bound to Aβ fibrils because of the changes in the rotational freedom of the carbon–carbon bond between the benzothiazole and aniline rings (Figure 2A) (18,21,22). In the unbound state, the ultrafast twisting dynamics around this bond are thought to cause rapid self-quenching of the excited state, resulting in low emission. However, upon binding to fibrils, the rotational freedom is apparently restricted and the excited state is readily populated. This concept was recently confirmed using a series of synthetic ThT analogs, which varied in their flexibility (22). The practical outcome of this mechanism is that ThT and its analogs can be used to spectroscopically quantify the amount of amyloid in a sample.

Binding modes of ThT to amyloid fibrils

The dramatic response of ThT's fluorescence to amyloids suggests that a defined binding event takes place to restrict the motion of the compound. Thus, studying this interaction would be expected

to reveal insights into the local amyloid topology and its molecular features. This strategy has been productive, with solid-state NMR (10), radiolabeling (23,24), competition assays (25), and molecular dynamics (MD) simulations (26–28) all having been used to evaluate ThT binding to amyloids. One of the first important observations was made by LeVine (25), who proposed that there are multiple binding sites for ThT on amyloids. Lockhart *et al.* (23) further refined this model using fluorescence and radiolabel-based assays. Together, these studies suggested the presence of three distinct binding sites (BS1, BS2, and BS3) on Aβ fibrils. Sites BS1 and BS2 are relatively abundant, with approximately one site per 4–35 Aβ monomers (Figure 2B). The less-abundant site, BS3 is found at approximately one site for every 300 monomers. Based on Forster resonance energy transfer measurements, binding sites BS1 and BS2 are thought to be in close proximity; however, occupancy was found to be neither cooperative nor competitive.

Further insights into how ThT binds in these different sites was supplied by MD simulations (27,28). Briefly, Wu *et al.* (27) simulated ThT binding to protofibrils composed of Aβ (16–22) and characterized the formation of three unique, populated clusters. Consistent with their earlier findings (28), the least populated binding cluster was located at the end of the protofibril in an orientation anti-parallel to the fibril axis. The two other clusters were more heavily populated and located parallel to the fibril axis (anti-parallel to the β-sheet). Together, these results seem to confirm Lockhart's model of two high-density ThT sites (BS1 and BS2) and a single low-density site (BS3) (Figure 2B). In this model, BS1 and BS2 are composed of surface grooves created by aligned side chains in the fibril axis, which provide much of the binding energy. When bound in these grooves, MD simulations suggest that the ring systems adopt a planar organization, with the charged nitrogen exposed to solvent (26,29) (Figure 2C). Interestingly, similar grooves have been proposed in amyloid fibrils composed of many different proteins (e.g. α-synuclein and prions), which may explain why ThT fluorescence is also sensitive to other, unrelated amyloids. However, because different amyloid-forming peptides do not share a high sequence identity, these results also suggest that some degenerative feature(s), such as hydrophobicity or contacts with the peptide backbone, are responsible for ThT binding.

Consistent with this idea, a closer examination of the molecular models reveals interesting features of the two most populated ThT binding sites (Figure 2C) (27). These two binding channels are lined with at least five, spatially consecutive, hydrophobic (Phe only or Phe and Val) side chains, which are located on opposite 'faces' of the amyloid structure. Similar findings have been observed by Koide *et al.*, who developed peptide self-assembly mimics that have repetitive, β-sheet amyloid-like structure (30–32). These soluble model proteins are amenable to crystallization, and co-crystals with bound ThT revealed that the compound binds in channels lined with five or six aromatic and hydrophobic side chains (31). Interestingly, it is critical that the favorable, hydrophobic residues within the channel are spatially consecutive, as two adjacent clusters of Tyr residues separated by a Lys and Glu showed no ThT binding (31). Collectively, these observations converge on a model in which five, aligned aromatic and/or hydrophobic residues are critical for ThT binding, while the exact identities of the side chains appear to be less important than their overall hydrophobicity.

An alternative binding mode was suggested by Groenning *et al.* using spectroscopy and molecular modeling to examine ThT binding to insulin fibrils. Although they confirmed that at least two distinct binding sites exist, with ThT binding predominantly parallel to the fibril axis (33,34), they further suggest that two ThT molecules in an excited-state dimer, or 'excimer,' form might bind to the grooves. Thus, a higher-order form of ThT, even as large as a micelle (35), might be involved in binding under some conditions and for some amyloids.

ThT also recognizes prefibrillar Aβ aggregates

As mentioned previously, prefibrillar intermediates are now thought to correlate with neurodegeneration, which has prompted interest in evaluating ThT binding to these structures. In the literature, there was initially debate over whether ThT binds oligomers and protofibrils. In fact, several groups initially defined ThT as a fibril-specific probe (36–39). However, methods for preparing prefibrillar structures have become more reliable, and comprehensive studies have now noted clear changes in fluorescence when ThT is added to prefibrils (40–42). For example, Walsh *et al.* (42) prepared samples of protofibrils and observed that they produce a concentration-dependent increase in ThT fluorescence. The binding of ThT to prefibrils is consistent with the binding information discussed earlier, as these structures are known to be rich in the hydrophobic, β-sheet content important for binding (42). For example, models of Aβ protofibrils have the requisite stretch of aligned hydrophobic residues one might expect to form the high-abundance ThT-binding site (43). However, fibrils and prefibrils are not identical in their binding to ThT, as many groups have noted that the maximum fluorescence induced by prefibrils is less (per mole of Aβ) than that stimulated by fibrils. For example, ThT fluorescence is modestly increased (1.5-fold) in the presence of Aβ oligomers (41) of either 1–40 or 1–42 Aβ (40), while fibrils often yield over 100-fold improvements in fluorescence (44). Moreover, using surface plasmon resonance (SPR), ThT (K_d = 498 nM) was shown to bind Aβ oligomers, but the total number of bound molecules was significantly less than in fibrils (40). These observations and others are likely consistent with other findings, because protofibrils are proposed to be more dynamic (45) and contain relatively fewer ThT-binding sites (46,47).

Interactions of ThT analogs with Aβ

Additional insights into the nature of the ThT-binding groove can be gained from studying synthetic ThT derivatives in which the molecular features of the molecule are systematically varied. In general, these derivatives are composed of a benzothiazole ring system attached to a substituted aniline (Figure 2A). Derivatives of this scaffold tend to have modifications at the amine of the aniline and at positions around the benzothiazole. Fortunately, many analogs have been explored as part of studies to develop imaging agents and; in many cases, the binding affinity of these compounds for amyloids has been reported. For example, Klunk *et al.* (48) synthesized several neutral ThT analogs, such as BTA-1, to explore the

effect of the positive charge on the benzothiazole ring (Figure 2A). They found that each neutral analog bound better to Aβ than ThT, with the best having a 40-fold improved affinity. These findings suggest that the positive charge in ThT may be detrimental for binding, which is a model supported by MD simulations indicating that the neutral BTA-1 is able to bind deeper into the hydrophobic binding grooves (27). However, ThT does not entirely compete with BTA-1 for binding (25), and Lockhart *et al.* (23) observed different binding patterns between the two ligands. *In silico* data further reveal that the ring systems of BTA-1 are planar in the bound orientation, instead of in a slightly twisted orientation, as observed with the charged ThT scaffold (27). Collectively, these data support a model in which some of the 'ThT binding sites' (i.e. BS1, BS2 and BS3) are more favorable for ThT, while others prefer neutral ligands. Interestingly, removal of the positive charge does not seem to affect oligomer binding, suggesting that one of the binding sites may be more prevalent in prefibrils (49). One possibility is that some of the sites allow deeper binding grooves, perhaps permitting neutral ligands with increased access. This idea is supported by measurements of the dimensions of the two sites identified by modeling: one has an average depth (backbone to solvent) of 5.4 Å, while the other is 7.1 Å. This deeper site might allow better penetration of neutral derivatives and, consequently, more favorable buried surface area and better affinity. These sites are unique in other dimensions as well; the shallower site is wider (17 Å), while the deeper site is narrower (10 Å). It is not yet clear which site is BS1 or BS2, but these differences support the model that the two sites have distinct properties. To our knowledge, structure-guided design has not yet been used to rationally exploit these differences.

Synthetic ThT derivatives have also been useful in further refining the features of the binding sites. For example, the benzothiazole can be replaced by a roughly planar benzofuran, imidazo-pyridine, imidazole, or benzoxazole core, without impacting affinity (49–52). Additionally, the aniline may be replaced with other flat, rigid moieties (e.g. stilbene and cyanobenzyl) without significant consequence (53,54). Insertion of a planar styrene group between the benzothiazole and aniline is also well tolerated (53), while some substitutions, such as bithiophenes, even improve affinity (55). In addition, these substitutions need not be aromatic, because methyl-piperazine groups appended to the aniline are tolerated (56). Interestingly, some of these substitutions extend the end-to-end distance of the ThT-like molecule by over 25%, suggesting that the binding channel can accommodate relatively long molecules, as long as they are planar and hydrophobic. However, there are limitations to the size of this channel, because installation of a large, freely rotatable rhenium chelate to the aniline abolishes binding (57). Appending the same group to the opposite end of the molecule actually enhanced binding by eightfold, which suggests that the dimensions of the channel are limited in some regions.

More subtle substitutions to the benzothiazole and aniline groups also help define the nature of the ThT binding site(s). For instance, the di-methyl amine group can be moved to the benzothiazole on the opposite side of the molecule without any consequence to binding affinity (58), suggesting that ThT derivatives may be able to bind in either orientation (Figure 2D). However, small alkyl-type substitutions in key positions appear to impact the binding mode (59). For example, a methyl group at the six-position of the benzothiazole ring is favored only if no methyl substitutions are present on the amine of the aniline (K_i = 9.5 nM). Alternatively, two methyl groups on this amine were favored if the six-position was hydrogen (K_i = 4 nM). Interestingly, a more polar, hydroxyl at the six-position was tolerated only if the aniline was substituted with at least one methyl group, suggesting that overall hydrophobicity is a critical element for binding.

In summary, multiple experiments have converged on a model in which amyloids contain up to three different binding sites. The two major sites (BS1 and BS2) are parallel to the fibril axis and are sensitive to relatively modest increases in steric size in some positions, while they can be readily elongated in the channel if overall planarity is maintained (Figure 2D). The major contacts with ThT are through aromatic and/or hydrophobic side chains in the parallel groove, and neutral derivatives bind tighter than their charged counterparts. It is important to note that BS1 and BS2 are present in roughly equivalent numbers (at least on fibrils) and that the experiments discussed here often focus on the composite affinities. Differences in the way that ThT derivatives bind the different sites might easily be masked in these studies and, moreover, little is likely learned about the requirements at BS3 in these types of experiments.

Congo Red

CR binds at least two sites on amyloids

Congo Red staining serves as a positive indicator of amyloid deposition, and its optical properties have been extensively reviewed (60,61). Briefly, CR selectively stains amyloid *in vitro* and in brain slices, and bound material displays a characteristic birefringence under polarized light. Like ThT, binding is observed with both Aβ-derived amyloids and amyloids derived from other peptides, suggesting that shared elements, such as β-sheet structure or peptide backbone, are involved in binding. Consistent with this idea, molecular docking simulations suggest that CR binds one site parallel to the fibril axis (anti-parallel to the β-sheets) (62) on amyloid fibrils (28,63,64) and protofibrils (28). Based on the approximate length one of the CR molecule (~19 Å) (Figure 3A), Klunk *et al.* (62) proposed a model in which it requires at least five Aβ monomers for binding. Lockhart *et al.* further characterized the number and types of CR-binding sites using a close analog, BSB (24). These studies revealed two non-equivalent binding sites, one of which is shared by ThT and is present at one site per three Aβ monomers. Moreover, the shared binding site was found to be the highest-density ThT binding site (BS2) (Figure 3B). These findings clarify the seemingly contradictory, earlier observations that CR and ThT have discrete binding sites (56), while other groups have reported competition (25,65). To keep consistent with the existing nomenclature and as a useful tool for discussion in this review, we identify the unique CR-binding site as BS4. Insight into the nature of BS4 came from studies on a prion-derived, amyloidogenic peptide with the sequence GNNQQNY (28). Specifically, MD simulations revealed that CR favors binding parallel to the fibril axis (anti-parallel to the β-sheets), but that it also populates a second site at the 'end' of the protofibril in an orientation anti-parallel to the fibril axis and parallel to the β-sheets (Figure 3C). This latter mode only

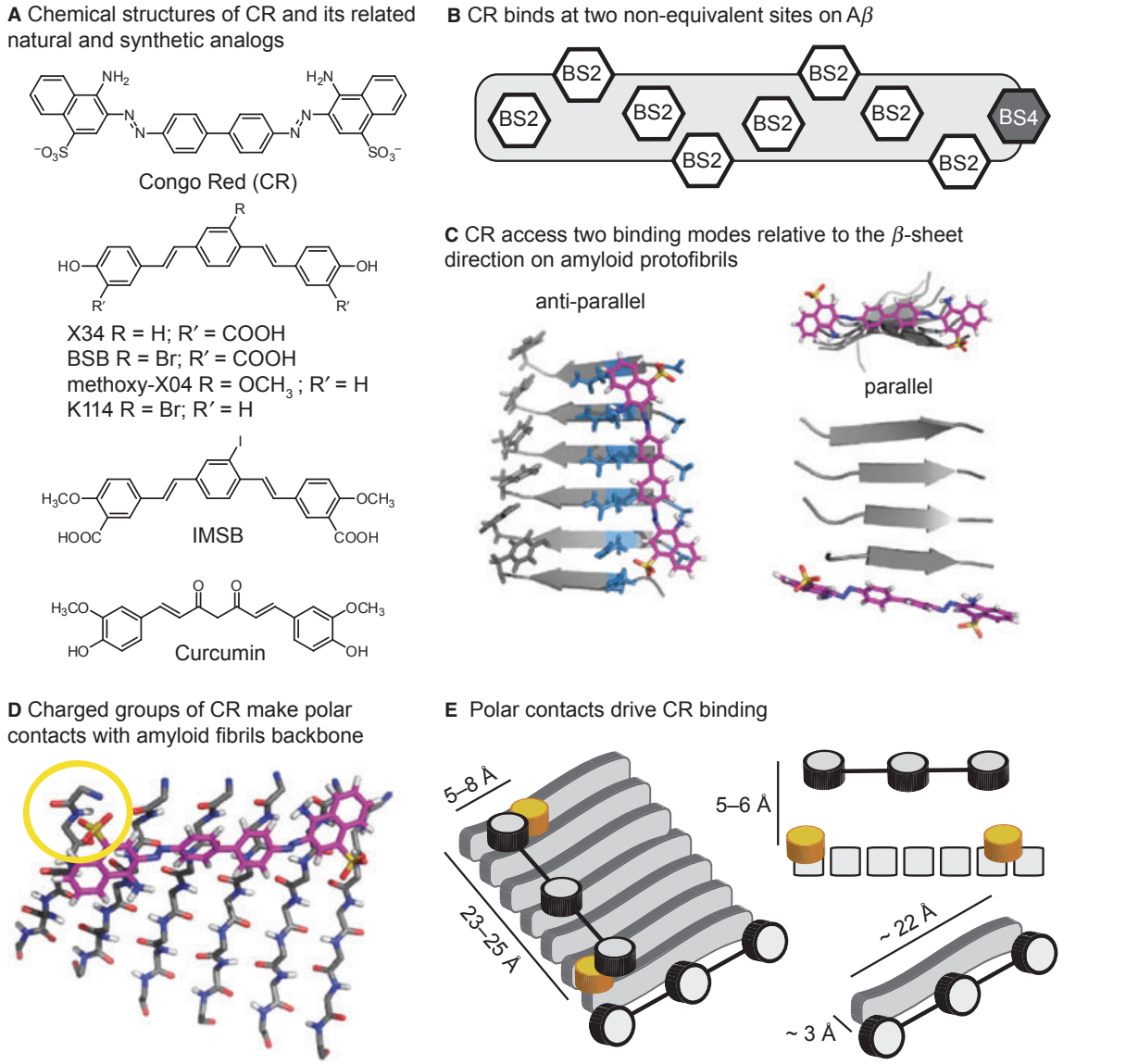

Figure 3: Congo red (CR) accesses two distinct binding sites on amyloids. (A) Structures of CR and its analogs. (B) The two CR binding sites on amyloid are shown, one with high density (BS2) and the other with low density (BS4). (C) Model of the high-density site, parallel to the fibril axis, and the low-density site at the end of the fibril. In the high-density site (BS2), the channel is largely composed of polar, uncharged residues. (D) Close-up of the BS2 site, highlighting the interaction with the charged sulfonic acid at the end of the CR molecule. Adapted from (28). (E) Schematic model of bound CR in the BS2 site, with the molecular dimensions and features shown.

represented approximately 11% of the total CR binding clusters, while the anti-parallel orientation was clearly preferred (78% of the total binding). This model perhaps explains the difference between CR binding affinity (K_d high nM – low μM) and its inhibition capacity (IC_{50} mid-high μM). In other words, CR may preferentially bind anti-parallel to the β-sheet, but this binding mode is not likely to inhibit fibril extension. When BS2 becomes saturated, CR may bind BS4 at the face of the growing fibril, only then disrupting monomer acquisition and elongation.

Similar to ThT, the main CR binding mode appears to be defined by a channel formed from side chains. The CR-binding channel is longer (23–25 Å) and narrower (5–8 Å) than the ThT channels, although it must include a portion of ThT-binding BS2 site based on the competition results. However, in contrast to the ThT channel, the residues that line the CR-binding site are largely polar and non-aromatic, such as Asn and Gly. In addition, despite the presence of nearby tyrosines, these aromatic residues do not appear to participate in CR binding (Figure 3C, left). Instead, in three of the four most populated clusters, the sulfonic acid moieties were aligned with the N-terminus, the only positive charge on the specific peptide used in these experiments (Figure 3D). These data suggest that ionic or polar interactions may be important for CR binding. Even greater detail has been provided by molecular docking of CR to 20

NMR structures (66) composed of near full-length Aβ (9–40) (67). These results confirmed two distinct CR binding sites, one located near Lys28 and the other at the C-terminus, making contacts with Asn27 and Val39. This is one of the first studies to implicate specific residues of the Aβ peptide in CR binding and, further, the contacts with Lys28 and Asn27 were confirmed by mutagenesis. Accordingly, these results suggest that, in the context of full length Aβ, Lys28 may provide the requisite positive charge to interact with the sulfonic acids. Thus, the identity of the side chains seems to play less of a role than polar contacts at the termini of the pocket.

CR binds prefibrillar amyloids

The first indication that CR may recognize prefibrils was by Walsh *et al.*, (42) who showed that CR absorbance was altered by Aβ protofibrils. In addition, CR and BSB have been found to bind globular Aβ oligomers (K_d = 3.2–19.5 μM) by SPR (40). Interestingly, solution-state NMR has recently revealed that CR binds low-molecular-weight Aβ species as well (68). It is not yet clear whether the fundamental features of the CR binding site(s) on early Aβ oligomers are similar to those defined for fibrils. However, similar to what has been observed with ThT, the absolute number of binding sites appears to be reduced compared with fibrils.

CR analogs reveal features of the amyloid-binding sites

Synthetic CR derivatives have provided further insight into the features of the binding sites on amyloids. For example, early analogs explored the requirements for the sulfonic acids (62). Using a radiolabeled displacement assay, Klunk *et al.* (62) identified that other charged groups, such as carboxylic acids, could replace the sulfonic groups. More recent studies found that the carboxylates were not absolutely required if phenolic hydroxyls were included (69). Further structure–activity relationship studies revealed that the methoxy substitutions that are located on some CR analogs are expendable (56,70); thus, there are likely no specific contacts made with those groups.

In addition to the contacts at the termini, the overall planarity of the molecules appears to be critical to their binding. Effective CR analogs, including X34 (71), BSB (72), K114 (73), IMSB (56), and methoxy-X04 (74), are all aromatic and planar and they seem to share binding sites (73) (Figure 3A). Other derivatives, based on the curcumin scaffold, revealed that two terminal aromatics are necessary (70). Interestingly, the overall size of the molecule was found to follow strict requirements, with the linker length restricted to 8–16 Å and including no more than 2–3 rotatable bonds. This general conclusion is supported by studies that indicate the more rigid enol form of curcumin is favored to bind Aβ, relative to the more flexible keto form (75,76). Together, these findings are consistent with a model in which the binding site for CR has limited size, with a hydrophobic channel and polar (or positively charged) groups at the ends (Figure 3D). These same molecular contacts may be equally crucial in prefibrillar conformations, because curcumin also inhibits the formation of low-molecular-weight (LMW) and oligomeric Aβ (77).

Peptides

The hydrophobic core region (HCR) is critical for Aβ aggregation

The HCR of Aβ spans residues 16–20 (KLVFF) and is thought to be one of the most critical elements for Aβ self-assembly (Figure 4A). This model arose from experiments, such as those reported by Tjernberg *et al.*, (78) in which they tested binding of Aβ peptides to full-length Aβ (1–40) and found that only three truncations (residues 10–19, 11–20, or 12–21) were capable of significant binding. Further studies showed that systematic substitution of the hydrophobic residues 17–20 in Aβ (10–42) for more hydrophilic amino acids reduces fibril formation (79). Moreover, point mutations in Val18, Phe19, and Phe20 are sufficient to block aggregation (79,80), suggesting that these residues play a particularly important role. Further, the hydrogen-bond network associated with the amide backbone of KLVFF is critical in determining aggregate morphology (81). Together, these findings suggest that the HCR, and especially KLVFF, may be an attractive target for probe development.

KLVFF motifs are aligned in Aβ fibrils and free sites are available at the 'ends'

Mature fibrils have a largely parallel β-sheet structure, such that the residues in this region are aligned (e.g. Phe 19 from one strand is stacked against Phe 19 from the next monomer) (Figure 4B). Even in prefibrillar samples, which contain both parallel and anti-parallel β-sheets (82,83), KLVFF regions are thought to be partially aligned, especially at the core Phe19 residue (84,85). These observations suggest that free KLVFF peptides will tend to align with their corresponding residues in both prefibrillar and fibrillar amyloids. Consistent with this idea, early structure–activity studies revealed that the peptides KLVFF, QKLVFF, HQKLVFF, KLVFFA, KLVFFAE, and QKLVFFA bound with the best affinity to Aβ (1–40) fibrils (86). This hypothesis was later confirmed using 38 fluorescently labeled 5-mer fragments (87). Interestingly, Ma and Nussinov (63) found that KLVFF interacts within Aβ oligomers in two orientations; one in which KLVFF binds its identical, homologous residues on the neighboring molecule, and other in which this directionality is reversed and shifted (Figure 4C).

Another critical feature of the KLVFF-binding site is that it will be exposed at the 'ends' of aggregates (Figure 4D). Indeed, extensive hydrogen–deuterium exchange (HDX) and solution-state NMR studies have shown that these residues are poorly solvent accessible in the core of fibrils (83,88,89) while they are more exposed in prefibrillar species. For example, only Leu17 and Val18 within the HCR are buried in LMW Aβ and only Leu17, Val18, and Phe19 In globular oligomers (88). Thus, opposite to what was discussed for the ThT- and CR-binding sites, there may be more KLVFF-binding sites in early amyloid species (11). Moreover, in the context of this review, these observations are of particular interest because they suggest that KLVFF-based probes might be used to understand the chemical and structural environment around the free 'ends' of amyloids. As discussed earlier, ThT- and CR-like ligands populate this region (BS3 and BS4), but with low abundance and weak affinity.

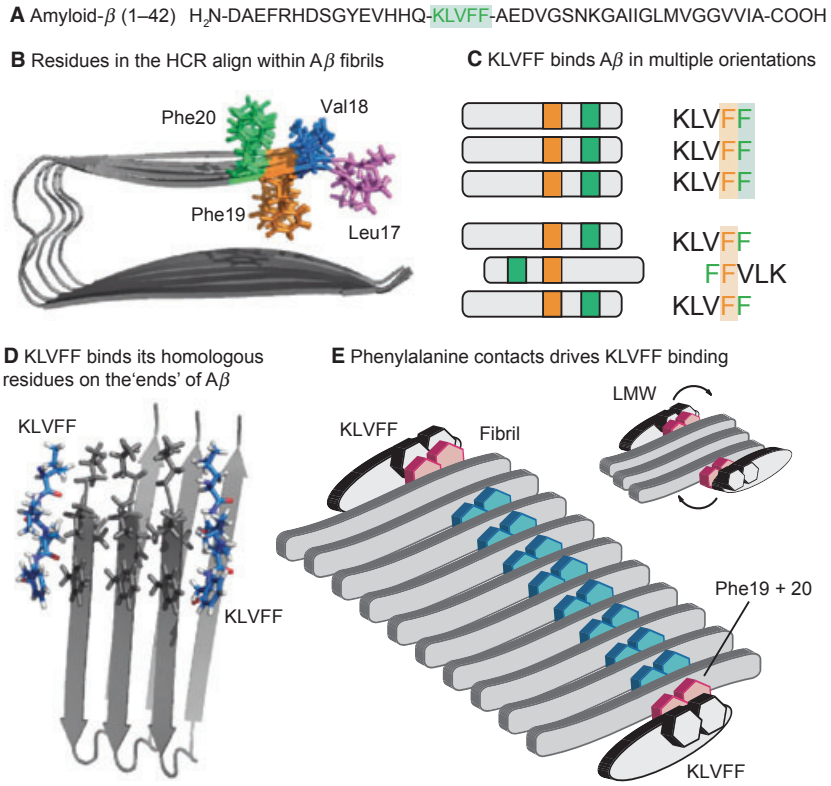

Figure 4: KLVFF bind at the exposed 'ends' of amyloid-β (Aβ) aggregates. (A) The sequence of Aβ (1–42), with the HCR highlighted in green. (B) The side chains of the KLVFF (colored) align within the stacked β-sheets of fibrils, leaving one motif free at each end. (C) KLVFF interacts with amyloids in two orientations; either the homologous residues align (left) or the sequence is reversed and shifted (right). The parallel mode is favored in fibrils, while the anti-parallel orientation predominates in non-fibrillar oligomers. Regardless, Phe-Phe contacts seem to be crucial for binding. (D) Model of KLVFF aligned with its cognate sequence in a fibril. Adapted from solid-state NMR structures (PDB:2BEG) (13). (E) Schematic model illustrates that KLVFF binds at the ends of fibrils and smaller oligomers (inset), with Phe residues being critical to the assembly. In smaller oligomers, KLVFF might bind anti-parallel to its cognate sequence.

Interactions of KLVFF derivatives with Aβ

Because the natural KLVFF sequence aligns with itself in amyloids, structure–activity studies on modified peptides can be used to probe the structural requirements in this region. For example, Cairo *et al.* (90) used SPR to determine the affinity of 24 KLVFF-based ligands for fibrils. They discovered that KLVFF has a low binding affinity (K_d = 1.4 mM), consistent with its inability to inhibit aggregation (91,92). The specific requirement for aromatic side chains was demonstrated by the 10-fold loss in affinity upon removal of the terminal Phe residue and the threefold loss in affinity upon replacement of Phe with His residues (KLVFH and KLVHH). In contrast, systematic substitution of the Phe residues for Tyr (KLVYF and KLVFY) did not dramatically alter affinity (K_d = 1.6–2.4 mM). However, there appears to be limits to these substitutions because introduction of a Trp residue (KLVFW) or two Tyr residues (KLVYY) was not well tolerated. Interestingly, the all D-KLVFF stereoisomer shows no difference in binding affinity (90,93), suggesting that the identity and order of the residues is more important than their position relative to the backbone. Consistent with this idea, substitution of the amide bond with either ester or *N*-methyl groups has little effect (94–96). Collectively, these findings suggest that the side chains of KLVFF are critical for recognition, but that the backbone does not significantly participate in binding of free peptide.

Although the core KLVFF sequence itself is somewhat sensitive to relatively minor changes, additions to either end seem well tolerated. For instance, appending polar residues, including stretches of lysines or arginines ($KLVFFK_4$, $KLVFFK_6$, and $KLVFFR_6$) significantly improves affinity (K_d = 37–80 μM) (90). It seems likely that these residues make favorable contacts with residues adjacent to the HCR to add additional binding energy. Further, the addition of the lysines was preferred on the C-terminal end of the molecule, as $KLVFFK_4$ displayed nearly a fivefold better affinity than K_4LVFF. Similarly, addition of bulky moieties to the N-terminus of KLVFF are tolerated, and, in some cases, improve recognition. For example, replacement of the lysine of KLVFF with a sterol had no effect on Aβ binding (97) and Gordon *et al.* (96) showed that an N-terminal anthranilic acid improves binding fivefold.

Together, these studies lead to a model in which KLVFF binds to sites at the ends of amyloids in either a parallel or anti-parallel mode (Figure 4E). The side chains, specifically the Phe residues, predominantly drive binding, with little contribution from the peptide backbone. Further, polar and non-polar groups could be appended to KLVFF to enhance its binding. In this regard, KLVFF may be a useful 'anchor' molecule for probing the surrounding regions at the ends of Aβ aggregates.

Conformation-Specific Probes

Aβ assembles into amyloids with a variety of distinct conformations

Extensive NMR (83,98,99), microscopy (100–102), HDX (45,83,88,103), Fourier-transform infrared spectroscopy (82,104), stability measurements (105), and MD (11,63) studies have suggested that Aβ can form multiple types of amyloid structures, including LMW (e.g. dimers, trimers, etc.) structures, soluble oligomers, protofibrils and fibrils. These structures differ in their overall size, shape, and the number of monomers they contain. In addition, a major theme in recent reports is that fibrils tend to be densely packed, while prefibrillar conformations are 'looser' or more dynamic in structure. For example, Wetzel's group showed that the core of Aβ fibrils is extremely resistant to solvent exchange (103), while Qi *et al.* (45) demonstrated that oligomers incorporate deuterium at a rate 10-fold greater than fibrils. These types of studies have also carefully mapped the residues in oligomers that are most accessible (83,88). Based on these structural differences, it seems likely that small molecules might be able to exploit the unique structural features that differentiate conformers. Consistent with this idea, numerous studies have reported small molecules that specifically block the formation of one type of amyloid conformation, without impacting others (106–109).

Conjugated polymers respond to Aβ conformation

Nilsson *et al.* and Hammarstrom *et al.* have performed pioneering studies using luminescent-conjugated polymers (LCPs) to selectively detect amyloids (110–114) (Figure 5A). When these polymers engage their target, they are designed to adopt a backbone orientation that conforms to the size and shape of the bound structure. This rearrangement aligns the polymer scaffold and alters the apparent fluorescence properties, yielding an 'optical fingerprint' specific to the bound amyloid. Using multiphoton microscopy, deposits in brain tissue have been labeled with several LCPs, revealing the presence of multiple, optically unique morphologies within a single plaque (113). Recent studies by these groups have also revealed smaller, pentameric thiophene derivatives (Figure 5A) that retain conformation-selective spectral binding properties (111). Included in these novel derivatives is the anionic ligand p-FTAA, which recognizes prefibrillar Aβ species *in vitro* and labels Aβ deposition in transgenic mouse models, indicating that these BBB-permeable derivatives may be informative for monitoring distinct conformations *in vivo* (111,112). It remains unclear precisely which Aβ conformations are bound by these probes or which ones correlate best with the toxic species. However, these findings do suggest that distinct amyloid morphologies co-localize in diseased brain tissue.

Indoles selectively detect prefibrillar amyloid

We recently reported an unbiased screening approach to identify compounds that interact with prefibrillar, but not fibrillar, amyloids (105,115). These efforts identified indole-based compounds that only undergo a change in fluorescence in the presence of prefibrillar structures, with a selectivity coefficient nearly 20-fold greater than ThT (Figure 5B). By optimizing the chemical structure of the indole and the reaction conditions (e.g. buffer and time), one promising probe, tryptophanol (TROL), was developed into a 'ThT-like' spectroscopic assay for prefibrillar amyloids (115). These findings suggest that some of the indoles access a site on prefibrillar Aβ that likely becomes buried or otherwise inaccessible upon fibril formation. Although the binding site and mechanism is not yet clear, these

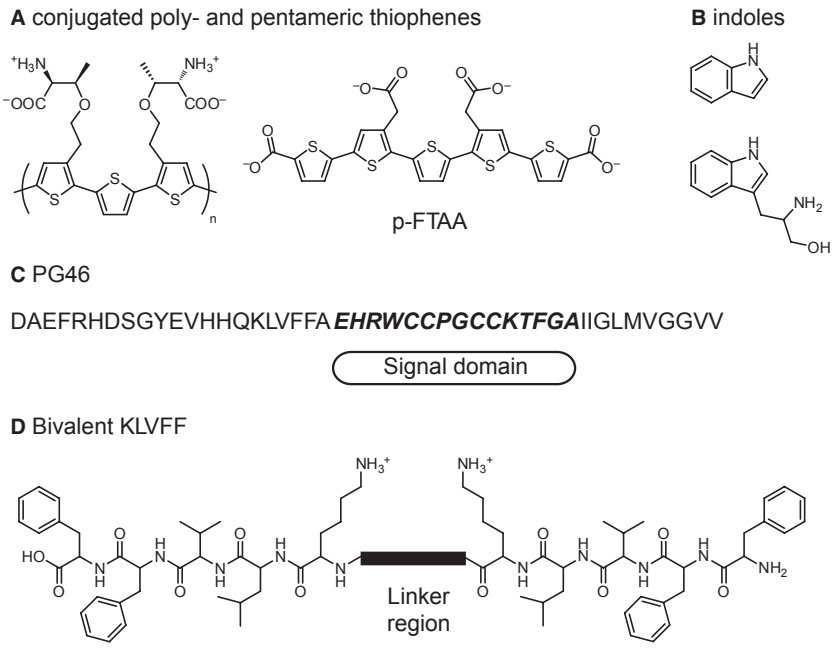

Figure 5: Chemical structures of some conformationally selective amyloid-β probes. The structures of various, reported molecules are shown. See the text for details.

probes further demonstrate that prefibrillar and fibrillar amyloids have different molecular features that can be exploited by small molecules.

Selective Aβ probes based on peptides

In addition to screening approaches, rational design has been used to develop conformationally sensitive probes. For example, Hu *et al.* (116) developed a peptide-based probe, PG46, in which a portion of the Aβ (1–40) was replaced with a binding epitope for the fluorescent dye, FLaSH (Figure 5C). When this modified peptide was added to different amyloids, they found that its fluorescence was only sensitive to intermediate aggregates (e.g. oligomers), but not LMW or fibrillar amyloids, likely because of differences in the local environment of the fluorophore. In addition, we recently developed bivalent KLVFF derivatives that specifically bind LMW trimers and tetramers of Aβ (117) (Figure 5D). Using molecular modeling, we estimated the distances between exposed KLVFF binding sites on the 'ends' of Aβ dimers, trimers, and tetramers. Then, corresponding ligands were assembled by solid-phase peptide chemistry with L-amino acids and a biotin tag was incorporated. Using polyacrylamide electrophoresis, we found that the bivalent KLVFF probes bound primarily to the trimer and tetramer, with some binding to dimer. These findings are consistent with recent MD simulations, which suggest that the Aβ (9–42) dimer is highly dynamic and may exist in orientations that are distinct from other conformations (11). In addition, no binding to monomers or higher-order oligomers was observed. Although in its infancy, the field of conformational selective probes holds promise in understanding amyloid structure and function.

Conclusions and Prospectus

Classic amyloid probes like ThT and CR have played a key role in our understanding of amyloid structure. As the appreciation of the number of different conformations has broadened, these scaffolds have found exciting, new roles. However, the classic probes tend to have relatively poor selectivity. Thus, the development of next-generation ligands will be an important step in further accelerating our understanding of the roles of amyloids in disease. Toward that goal, one approach that might be particularly fruitful is the use of multivalent ligands. The synthesis of bivalent, 'molecular tweezers' that bind amyloids have been reported (92,93,117–121), and we expect that these types of scaffolds may be incorporated into the next battery of tools. In turn, these designed ligands might be used to ask the next generation of questions about amyloid structure and function. Where are the small molecule-binding sites positioned in relation to one another? How does the position or number of these sites change upon transition from one conformation to another? A combination of old and new chemical probes will likely be necessary to answer these questions and others.

Acknowledgments

We thank Professor Yong Duan of UC-Davis for kindly allowing access to PDB files of docked ThT and CR molecules and Dr Harvey Swick for reading the manuscript. Our work on amyloid ligands is funded by the Alzheimer's Association (NIRG 89471 and IIRG 60067). A.A.R. was supported by a predoctoral fellowship from the NIH/NIA Biogerontology Training Grant (AG000114).

References

1. Dahlgren K.N., Manelli A.M., Stine W.B. Jr, Baker L.K., Krafft G.A., LaDu M.J. (2002) Oligomeric and fibrillar species of amyloid-beta peptides differentially affect neuronal viability. J Biol Chem;277:32046–32053.
2. Shankar G.M., Li S., Mehta T.H., Garcia-Munoz A., Shepardson N.E., Smith I., Brett F.M., Farrell M.A., Rowan M.J., Lemere C.A., Regan C.M., Walsh D.M., Sabatini B.L., Selkoe D.J. (2008) Amyloid-beta protein dimers isolated directly from Alzheimer's brains impair synaptic plasticity and memory. Nat Med;14:837–842.
3. Gong Y., Chang L., Viola K.L., Lacor P.N., Lambert M.P., Finch C.E., Krafft G.A., Klein W.L. (2003) Alzheimer's disease-affected brain: presence of oligomeric A beta ligands (ADDLs) suggests a molecular basis for reversible memory loss. Proc Natl Acad Sci USA;100:10417–10422.
4. Klyubin I., Walsh D.M., Lemere C.A., Cullen W.K., Shankar G.M., Betts V., Spooner E.T., Jiang L., Anwyl R., Selkoe D.J., Rowan M.J. (2005) Amyloid beta protein immunotherapy neutralizes Abeta oligomers that disrupt synaptic plasticity *in vivo*. Nat Med;11:556–561.
5. Selkoe D.J. (2008) Soluble oligomers of the amyloid beta-protein impair synaptic plasticity and behavior. Behav Brain Res;192:106–113.
6. Ferreira S.T., Vieira M.N., De Felice F.G. (2007) Soluble protein oligomers as emerging toxins in Alzheimer's and other amyloid diseases. IUBMB Life;59:332–345.
7. Haass C., Selkoe D.J. (2007) Soluble protein oligomers in neurodegeneration: lessons from the Alzheimer's amyloid beta-peptide. Nat Rev Mol Cell Biol;8:101–112.
8. Klein W.L., Stine W.B. Jr, Teplow D.B. (2004) Small assemblies of unmodified amyloid beta-protein are the proximate neurotoxin in Alzheimer's disease. Neurobiol Aging;25:569–580.
9. O'Nuallain B., Freir D.B., Nicoll A.J., Risse E., Ferguson N., Herron C.E., Collinge J., Walsh D.M. (2010) Amyloid beta-protein dimers rapidly form stable synaptotoxic protofibrils. J Neurosci;30:14411–14419.
10. Balbach J.J., Ishii Y., Antzutkin O.N., Leapman R.D., Rizzo N.W., Dyda F., Reed J., Tycko R. (2000) Amyloid fibril formation by A beta 16–22, a seven-residue fragment of the Alzheimer's beta-amyloid peptide, and structural characterization by solid state NMR. Biochemistry;39:13748–13759.
11. Horn A.H., Sticht H. (2010) Amyloid-beta42 oligomer structures from fibrils: a systematic molecular dynamics study. J Phys Chem;114:2219–2226.
12. Klimov D.K., Thirumalai D. (2003) Dissecting the assembly of Abeta16–22 amyloid peptides into antiparallel beta sheets. Structure;11:295–307.
13. Luhrs T., Ritter C., Adrian M., Riek-Loher D., Bohrmann B., Dobeli H., Schubert D., Riek R. (2005) 3D structure of Alzhei-

mer's amyloid-beta(1–42) fibrils. Proc Natl Acad Sci USA;102:17342–17347.
14. Vassar P.S., Culling C.F. (1959) Fluorescent stains, with special reference to amyloid and connective tissues. Arch Pathol;68:487–498.
15. Naiki H., Higuchi K., Hosokawa M., Takeda T. (1989) Fluorometric determination of amyloid fibrils *in vitro* using the fluorescent dye, thioflavin T1. Anal Biochem;177:244–249.
16. Naiki H., Higuchi K., Matsushima K., Shimada A., Chen W.H., Hosokawa M., Takeda T. (1990) Fluorometric examination of tissue amyloid fibrils in murine senile amyloidosis: use of the fluorescent indicator, thioflavine T. Lab Invest;62:768–773.
17. Naiki H., Higuchi K., Nakakuki K., Takeda T. (1991) Kinetic analysis of amyloid fibril polymerization *in vitro*. Lab Invest;65:104–110.
18. Singh P.K., Kumbhakar M., Pal H., Nath S. (2009) Ultrafast torsional dynamics of protein binding dye thioflavin-T in nanoconfined water pool. J Phys Chem;113:8532–8538.
19. LeVine H. 3rd (1993) Thioflavine T interaction with synthetic Alzheimer's disease beta-amyloid peptides: detection of amyloid aggregation in solution. Protein Sci;2:404–410.
20. LeVine H. 3rd (1999) Quantification of beta-sheet amyloid fibril structures with thioflavin T. Methods Enzymol;309:274–284.
21. Singh P.K., Kumbhakar M., Pal H., Nath S. (2010) Ultrafast bond twisting dynamics in amyloid fibril sensor. J Phys Chem;114:2541–2546.
22. Srivastava A., Singh P.K., Kumbhakar M., Mukherjee T., Chattopadyay S., Pal H., Nath S. (2010) Identifying the bond responsible for the fluorescence modulation in an amyloid fibril sensor. Chemistry;16:9257–9263.
23. Lockhart A., Ye L., Judd D.B., Merritt A.T., Lowe P.N., Morgenstern J.L., Hong G., Gee A.D., Brown J. (2005) Evidence for the presence of three distinct binding sites for the thioflavin T class of Alzheimer's disease PET imaging agents on beta-amyloid peptide fibrils. J Biol Chem;280:7677–7684.
24. Ye L., Morgenstern J.L., Gee A.D., Hong G., Brown J., Lockhart A. (2005) Delineation of positron emission tomography imaging agent binding sites on beta-amyloid peptide fibrils. J Biol Chem;280:23599–23604.
25. LeVine H. 3rd (2005) Multiple ligand binding sites on A beta(1–40) fibrils. Amyloid;12:5–14.
26. Rodriguez-Rodriguez C., Rimola A., Rodriguez-Santiago L., Ugliengo P., Alvarez-Larena A., Gutierrez-de-Teran H., Sodupe M., Gonzalez-Duarte P. (2010) Crystal structure of thioflavin-T and its binding to amyloid fibrils: insights at the molecular level. Chem Commun (Camb);46:1156–1158.
27. Wu C., Wang Z., Lei H., Duan Y., Bowers M.T., Shea J.E. (2008) The binding of thioflavin T and its neutral analog BTA-1 to protofibrils of the Alzheimer's disease Abeta(16–22) peptide probed by molecular dynamics simulations. J Mol Biol;384:718–729.
28. Wu C., Wang Z., Lei H., Zhang W., Duan Y. (2007) Dual binding modes of Congo red to amyloid protofibril surface observed in molecular dynamics simulations. J Am Chem Soc;129:1225–1232.
29. Dzwolak W., Pecul M. (2005) Chiral bias of amyloid fibrils revealed by the twisted conformation of Thioflavin T: an induced circular dichroism/DFT study. FEBS Lett;579:6601–6603.
30. Biancalana M., Koide S. (2010) Molecular mechanism of Thioflavin-T binding to amyloid fibrils. Biochim Biophys Acta;1804:1405–1412.
31. Biancalana M., Makabe K., Koide A., Koide S. (2009) Molecular mechanism of thioflavin-T binding to the surface of beta-rich peptide self-assemblies. J Mol Biol;385:1052–1063.
32. Wu C., Biancalana M., Koide S., Shea J.E. (2009) Binding modes of thioflavin-T to the single-layer beta-sheet of the peptide self-assembly mimics. J Mol Biol;394:627–633.
33. Groenning M., Norrman M., Flink J.M., van de Weert M., Bukrinsky J.T., Schluckebier G., Frokjaer S. (2007) Binding mode of Thioflavin T in insulin amyloid fibrils. J Struct Biol;159:483–497.
34. Groenning M. (2009) Binding mode of Thioflavin T and other molecular probes in the context of amyloid fibrils-current status. J Chem Biol;3:1–18.
35. Khurana R., Coleman C., Ionescu-Zanetti C., Carter S.A., Krishna V., Grover R.K., Roy R., Singh S. (2005) Mechanism of thioflavin T binding to amyloid fibrils. J Struct Biol;151:229–238.
36. Gellermann G.P., Byrnes H., Striebinger A., Ullrich K., Mueller R., Hillen H., Barghorn S. (2008) Abeta-globulomers are formed independently of the fibril pathway. Neurobiol Dis;30:212–220.
37. Caspersen C., Wang N., Yao J., Sosunov A., Chen X., Lustbader J.W., Xu H.W., Stern D., McKhann G., Yan S.D. (2005) Mitochondrial Abeta: a potential focal point for neuronal metabolic dysfunction in Alzheimer's disease. FASEB J;19:2040–2041.
38. Lacor P.N., Buniel M.C., Chang L., Fernandez S.J., Gong Y., Viola K.L., Lambert M.P., Velasco P.T., Bigio E.H., Finch C.E., Krafft G.A., Klein W.L. (2004) Synaptic targeting by Alzheimer's-related amyloid beta oligomers. J Neurosci;24:10191–10200.
39. Oddo S., Caccamo A., Tran L., Lambert M.P., Glabe C.G., Klein W.L., LaFerla F.M. (2006) Temporal profile of amyloid-beta (Abeta) oligomerization in an *in vivo* model of Alzheimer disease. A link between Abeta and tau pathology. J Biol Chem;281:1599–1604.
40. Maezawa I., Hong H.S., Liu R., Wu C.Y., Cheng R.H., Kung M.P., Kung H.F., Lam K.S., Oddo S., Laferla F.M., Jin L.W. (2008) Congo red and thioflavin-T analogs detect Abeta oligomers. J Neurochem;104:457–468.
41. Ryan D.A., Narrow W.C., Federoff H.J., Bowers W.J. (2010) An improved method for generating consistent soluble amyloid-beta oligomer preparations for *in vitro* neurotoxicity studies. J Neurosci Methods;190:171–179.
42. Walsh D.M., Hartley D.M., Kusumoto Y., Fezoui Y., Condron M.M., Lomakin A., Benedek G.B., Selkoe D.J., Teplow D.B. (1999) Amyloid beta-protein fibrillogenesis. Structure and biological activity of protofibrillar intermediates. J Biol Chem;274:25945–25952.
43. Lemkul J.A., Bevan D.R. (2010) Assessing the stability of Alzheimer's amyloid protofibrils using molecular dynamics. J Phys Chem;114:1652–1660.
44. Jan A., Gokce O., Luthi-Carter R., Lashuel H.A. (2008) The ratio of monomeric to aggregated forms of Abeta40 and Abeta42 is an important determinant of amyloid-beta aggregation, fibrillogenesis, and toxicity. J Biol Chem;283:28176–28189.
45. Qi W., Zhang A., Patel D., Lee S., Harrington J.L., Zhao L., Schaefer D., Good T.A., Fernandez E.J. (2008) Simultaneous

monitoring of peptide aggregate distributions, structure, and kinetics using amide hydrogen exchange: application to Abeta(1–40) fibrillogenesis. Biotechnol Bioeng;100:1214–1227.
46. O'Nuallain B., Shivaprasad S., Kheterpal I., Wetzel R. (2005) Thermodynamics of A beta(1–40) amyloid fibril elongation. Biochemistry;44:12709–12718.
47. Shivaprasad S., Wetzel R. (2006) Scanning cysteine mutagenesis analysis of Abeta-(1–40) amyloid fibrils. J Biol Chem;281:993–1000.
48. Klunk W.E., Wang Y., Huang G.F., Debnath M.L., Holt D.P., Mathis C.A. (2001) Uncharged thioflavin-T derivatives bind to amyloid-beta protein with high affinity and readily enter the brain. Life Sci;69:1471–1484.
49. Zhuang Z.P., Kung M.P., Hou C., Plossl K., Skovronsky D., Gur T.L., Trojanowski J.Q., Lee V.M., Kung H.F. (2001) IBOX(2-(4′-dimethylaminophenyl)-6-iodobenzoxazole): a ligand for imaging amyloid plaques in the brain. Nucl Med Biol;28:887–894.
50. Kung M.P., Hou C., Zhuang Z.P., Zhang B., Skovronsky D., Trojanowski J.Q., Lee V.M., Kung H.F. (2002) IMPY: an improved thioflavin-T derivative for *in vivo* labeling of beta-amyloid plaques. Brain Res;956:202–210.
51. Kung M.P., Zhuang Z.P., Hou C., Jin L.W., Kung H.F. (2003) Characterization of radioiodinated ligand binding to amyloid beta plaques. J Mol Neurosci;20:249–254.
52. Ono M., Kawashima H., Nonaka A., Kawai T., Haratake M., Mori H., Kung M.P., Kung H.F., Saji H., Nakayama M. (2006) Novel benzofuran derivatives for PET imaging of beta-amyloid plaques in Alzheimer's disease brains. J Med Chem;49:2725–2730.
53. Lee J.H., Byeon S.R., Lim S.J., Oh S.J., Moon D.H., Yoo K.H., Chung B.Y., Kim D.J. (2008) Synthesis and evaluation of stilbenylbenzoxazole and stilbenylbenzothiazole derivatives for detecting beta-amyloid fibrils. Bioorg Med Chem Lett;18:1534–1537.
54. Ono M., Hayashi S., Kimura H., Kawashima H., Nakayama M., Saji H. (2009) Push-pull benzothiazole derivatives as probes for detecting beta-amyloid plaques in Alzheimer's brains. Bioorg Med Chem;17:7002–7007.
55. Cui M.C., Li Z.J., Tang R.K., Liu B.L. (2010) Synthesis and evaluation of novel benzothiazole derivatives based on the bithiophene structure as potential radiotracers for beta-amyloid plaques in Alzheimer's disease. Bioorg Med Chem;18:2777–2784.
56. Zhuang Z.P., Kung M.P., Hou C., Skovronsky D.M., Gur T.L., Plossl K., Trojanowski J.Q., Lee V.M., Kung H.F. (2001) Radioiodinated styrylbenzenes and thioflavins as probes for amyloid aggregates. J Med Chem;44:1905–1914.
57. Lin K.S., Debnath M.L., Mathis C.A., Klunk W.E. (2009) Synthesis and beta-amyloid binding properties of rhenium 2-phenylbenzothiazoles. Bioorg Med Chem Lett;19:2258–2262.
58. Wang Y., Mathis C.A., Huang G.F., Debnath M.L., Holt D.P., Shao L. *et al.* (2003) Effects of lipophilicity on the affinity and nonspecific binding of iodinated benzothiazole derivatives. J Mol Neurosci;20:255–260.
59. Mathis C.A., Wang Y., Holt D.P., Huang G.F., Debnath M.L., Klunk W.E. (2003) Synthesis and evaluation of 11C-labeled 6-substituted 2-arylbenzothiazoles as amyloid imaging agents. J Med Chem;46:2740–2754.
60. Howie A.J., Brewer D.B. (2009) Optical properties of amyloid stained by Congo red: history and mechanisms. Micron;40:285–301.
61. Howie A.J., Brewer D.B., Howell D., Jones A.P. (2008) Physical basis of colors seen in Congo red-stained amyloid in polarized light. Lab Invest;88:232–242.
62. Klunk W.E., Debnath M.L., Pettegrew J.W. (1994) Development of small molecule probes for the beta-amyloid protein of Alzheimer's disease. Neurobiol Aging;15:691–698.
63. Ma B., Nussinov R. (2002) Stabilities and conformations of Alzheimer's beta -amyloid peptide oligomers (Abeta 16–22, Abeta 16–35, and Abeta 10–35): sequence effects. Proc Natl Acad Sci USA;99:14126–14131.
64. Childers W.S., Mehta A.K., Lu K., Lynn D.G. (2009) Templating molecular arrays in amyloid's cross-beta grooves. J Am Chem Soc;131:10165–10172.
65. Hudson S.A., Ecroyd H., Kee T.W., Carver J.A. (2009) The thioflavin T fluorescence assay for amyloid fibril detection can be biased by the presence of exogenous compounds. FEBS J;276:5960–5972.
66. Petkova A.T., Ishii Y., Balbach J.J., Antzutkin O.N., Leapman R.D., Delaglio F., Tycko R. (2002) A structural model for Alzheimer's beta -amyloid fibrils based on experimental constraints from solid state NMR. Proc Natl Acad Sci USA;99:16742–16747.
67. Keshet B., Gray J.J., Good T.A. (2010) Structurally distinct toxicity inhibitors bind at common loci on beta-amyloid fibril. Protein Sci;19:2291–2304.
68. Pedersen M.O., Mikkelsen K., Behrens M.A., Pedersen J.S., Enghild J.J., Skrydstrup T., Malmendal A., Nielsen N.C. (2010) NMR reveals two-step association of Congo Red to amyloid beta in low-molecular-weight aggregates. J Phys Chem;114:16003–16010.
69. Mathis C.A., Wang Y., Klunk W.E. (2004) Imaging beta-amyloid plaques and neurofibrillary tangles in the aging human brain. Curr Pharm Des;10:1469–1492.
70. Reinke A.A., Gestwicki J.E. (2007) Structure-activity relationships of amyloid beta-aggregation inhibitors based on curcumin: influence of linker length and flexibility. Chem Biol Drug Des;70:206–215.
71. Styren S.D., Hamilton R.L., Styren G.C., Klunk W.E. (2000) X-34, a fluorescent derivative of Congo red: a novel histochemical stain for Alzheimer's disease pathology. J Histochem Cytochem;48:1223–1232.
72. Skovronsky D.M., Zhang B., Kung M.P., Kung H.F., Trojanowski J.Q., Lee V.M. (2000) *In vivo* detection of amyloid plaques in a mouse model of Alzheimer's disease. Proc Natl Acad Sci USA;97:7609–7614.
73. Crystal A.S., Giasson B.I., Crowe A., Kung M.P., Zhuang Z.P., Trojanowski J.Q., Lee V.M. (2003) A comparison of amyloid fibrillogenesis using the novel fluorescent compound K114. J Neurochem;86:1359–1368.
74. Klunk W.E., Bacskai B.J., Mathis C.A., Kajdasz S.T., McLellan M.E., Frosch M.P., Debnath M.L., Holt D.P., Wang Y., Hyman B.T. (2002) Imaging Abeta plaques in living transgenic mice with multiphoton microscopy and methoxy-X04, a systemically administered Congo red derivative. J Neuropathol Exp Neurol;61:797–805.

75. Ortica F., Rodgers M.A. (2001) A laser flash photolysis study of curcumin in dioxane-water mixtures. Photochem Photobiol;74:745–751.
76. Yanagisawa D., Shirai N., Amatsubo T., Taguchi H., Hirao K., Urushitani M., Morikawa S. *et al.* (2010) Relationship between the tautomeric structures of curcumin derivatives and their Abeta-binding activities in the context of therapies for Alzheimer's disease. Biomaterials;31:4179–4185.
77. Yang F., Lim G.P., Begum A.N., Ubeda O.J., Simmons M.R., Ambegaokar S.S., Chen P.P., Kayed R., Glabe C.G., Frautschy S.A., Cole G.M. (2005) Curcumin inhibits formation of amyloid beta oligomers and fibrils, binds plaques, and reduces amyloid *in vivo*. J Biol Chem;280:5892–5901.
78. Tjernberg L.O., Naslund J., Lindqvist F., Johansson J., Karlstrom A.R., Thyberg J., Terenius L., Nordstedt C. (1996) Arrest of beta-amyloid fibril formation by a pentapeptide ligand. J Biol Chem;271:8545–8548.
79. Hilbich C., Kisters-Woike B., Reed J., Masters C.L., Beyreuther K. (1992) Substitutions of hydrophobic amino acids reduce the amyloidogenicity of Alzheimer's disease beta A4 peptides. J Mol Biol;228:460–473.
80. Esler W.P., Stimson E.R., Ghilardi J.R., Lu Y.A., Felix A.M., Vinters H.V., Mantyh P.W., Lee J.P., Maggio J.E. (1996) Point substitution in the central hydrophobic cluster of a human beta-amyloid congener disrupts peptide folding and abolishes plaque competence. Biochemistry;35:13914–13921.
81. Bieschke J., Siegel S.J., Fu Y., Kelly J.W. (2008) Alzheimer's Abeta peptides containing an isostructural backbone mutation afford distinct aggregate morphologies but analogous cytotoxicity. Evidence for a common low-abundance toxic structure(s)? Biochemistry;47:50–59.
82. Cerf E., Sarroukh R., Tamamizu-Kato S., Breydo L., Derclaye S., Dufrene Y.F., Narayanaswami V., Goormaghtigh E., Ruysschaert J.M., Raussens V. (2009) Antiparallel beta-sheet: a signature structure of the oligomeric amyloid beta-peptide. Biochem J;421:415–423.
83. Yu L., Edalji R., Harlan J.E., Holzman T.F., Lopez A.P., Labkovsky B., Hillen H. *et al.* (2009) Structural characterization of a soluble amyloid beta-peptide oligomer. Biochemistry;48:1870–1877.
84. Hwang W., Zhang S., Kamm R.D., Karplus M. (2004) Kinetic control of dimer structure formation in amyloid fibrillogenesis. Proc Natl Acad Sci USA;101:12916–12921.
85. Gnanakaran S., Nussinov R., Garcia A.E. (2006) Atomic-level description of amyloid beta-dimer formation. J Am Chem Soc;128:2158–2159.
86. Tjernberg L.O., Lilliehook C., Callaway D.J., Naslund J., Hahne S., Thyberg J., Terenius L., Nordstedt C. (1997) Controlling amyloid beta-peptide fibril formation with protease-stable ligands. J Biol Chem;272:12601–12605.
87. Watanabe K., Segawa T., Nakamura K., Kodaka M., Konakahara T., Okuno H. (2001) Identification of the molecular interaction site of amyloid beta peptide by using a fluorescence assay. J Pept Res;58:342–346.
88. Zhang A., Qi W., Good T.A., Fernandez E.J. (2009) Structural differences between Abeta(1–40) intermediate oligomers and fibrils elucidated by proteolytic fragmentation and hydrogen/deuterium exchange. Biophys J;96:1091–1104.
89. Olofsson A., Sauer-Eriksson A.E., Ohman A. (2006) The solvent protection of alzheimer amyloid-beta-(1–42) fibrils as determined by solution NMR spectroscopy. J Biol Chem;281:477–483.
90. Cairo C.W., Strzelec A., Murphy R.M., Kiessling L.L. (2002) Affinity-based inhibition of beta-amyloid toxicity. Biochemistry;41:8620–8629.
91. Chalifour R.J., McLaughlin R.W., Lavoie L., Morissette C., Tremblay N., Boule M., Sarazin P., Stea D., Lacombe D., Tremblay P., Gervais F. (2003) Stereoselective interactions of peptide inhibitors with the beta-amyloid peptide. J Biol Chem;278:34874–34881.
92. Ouberai M., Dumy P., Chierici S., Garcia J. (2009) Synthesis and biological evaluation of clicked curcumin and clicked KLVFFA conjugates as inhibitors of beta-amyloid fibril formation. Bioconjug Chem;20:2123–2132.
93. Zhang G., Leibowitz M.J., Sinko P.J., Stein S. (2003) Multiple-peptide conjugates for binding beta-amyloid plaques of Alzheimer's disease. Bioconjug Chem;14:86–92.
94. Gordon D.J., Meredith S.C. (2003) Probing the role of backbone hydrogen bonding in beta-amyloid fibrils with inhibitor peptides containing ester bonds at alternate positions. Biochemistry;42:475–485.
95. Gordon D.J., Sciarretta K.L., Meredith S.C. (2001) Inhibition of beta-amyloid(40) fibrillogenesis and disassembly of beta-amyloid(40) fibrils by short beta-amyloid congeners containing *N*-methyl amino acids at alternate residues. Biochemistry;40:8237–8245.
96. Gordon D.J., Tappe R., Meredith S.C. (2002) Design and characterization of a membrane permeable *N*-methyl amino acid-containing peptide that inhibits Abeta1–40 fibrillogenesis. J Pept Res;60:37–55.
97. Findeis M.A., Musso G.M., Arico-Muendel C.C., Benjamin H.W., Hundal A.M., Lee J.J., Chin J., Kelley M., Wakefield J., Hayward N.J., Molineaux S.M. (1999) Modified-peptide inhibitors of amyloid beta-peptide polymerization. Biochemistry;38:6791–6800.
98. Ahmed M., Davis J., Aucoin D., Sato T., Ahuja S., Aimoto S., Elliott J.I., Van Nostrand W.E., Smith S.O. (2010) Structural conversion of neurotoxic amyloid-beta(1–42) oligomers to fibrils. Nat Struct Mol Biol;17:561–567.
99. Chimon S., Shaibat M.A., Jones C.R., Calero D.C., Aizezi B., Ishii Y. (2007) Evidence of fibril-like beta-sheet structures in a neurotoxic amyloid intermediate of Alzheimer's beta-amyloid. Nat Struct Mol Biol;14:1157–1164.
100. Yagi H., Ban T., Morigaki K., Naiki H., Goto Y. (2007) Visualization and classification of amyloid beta supramolecular assemblies. Biochemistry;46:15009–15017.
101. Mastrangelo I.A., Ahmed M., Sato T., Liu W., Wang C., Hough P., Smith S.O. (2006) High-resolution atomic force microscopy of soluble Abeta42 oligomers. J Mol Biol;358:106–119.
102. Zhu M., Han S., Zhou F., Carter S.A., Fink A.L. (2004) Annular oligomeric amyloid intermediates observed by *in situ* atomic force microscopy. J Biol Chem;279:24452–24459.
103. Kheterpal I., Zhou S., Cook K.D., Wetzel R. (2000) Abeta amyloid fibrils possess a core structure highly resistant to hydrogen exchange. Proc Natl Acad Sci USA;97:13597–13601.

104. Sarroukh R., Cerf E., Derclaye S., Dufrene Y.F., Goormaghtigh E., Ruysschaert J.M., Raussens V. (2011) Transformation of amyloid beta(1–40) oligomers into fibrils is characterized by a major change in secondary structure. Cell Mol Life Sci;68:1429–1438.
105. Reinke A.A., Seh H.Y., Gestwicki J.E. (2009) A chemical screening approach reveals that indole fluorescence is quenched by pre-fibrillar but not fibrillar amyloid-beta. Bioorg Med Chem Lett;19:4952–4957.
106. Necula M., Breydo L., Milton S., Kayed R., van der Veer W.E., Tone P., Glabe C.G. (2007) Methylene blue inhibits amyloid Abeta oligomerization by promoting fibrillization. Biochemistry;46:8850–8860.
107. Necula M., Kayed R., Milton S., Glabe C.G. (2007) Small molecule inhibitors of aggregation indicate that amyloid beta oligomerization and fibrillization pathways are independent and distinct. J Biol Chem;282:10311–10324.
108. Convertino M., Pellarin R., Catto M., Carotti A., Caflisch A. (2009) 9,10-Anthraquinone hinders beta-aggregation: how does a small molecule interfere with Abeta-peptide amyloid fibrillation? Protein Sci;18:792–800.
109. Maezawa I., Hong H.S., Wu H.C., Battina S.K., Rana S., Iwamoto T., Radke G.A., Pettersson E., Martin G.M., Hua D.H., Jin L.W. (2006) A novel tricyclic pyrone compound ameliorates cell death associated with intracellular amyloid-beta oligomeric complexes. J Neurochem;98:57–67.
110. Aslund A., Herland A., Hammarstrom P., Nilsson K.P., Jonsson B.H., Inganas O., Konradsson P. (2007) Studies of luminescent conjugated polythiophene derivatives: enhanced spectral discrimination of protein conformational states. Bioconjug Chem;18:1860–1868.
111. Aslund A., Sigurdson C.J., Klingstedt T., Grathwohl S., Bolmont T., Dickstein D.L., Glimsdal E. *et al.* (2009) Novel pentameric thiophene derivatives for *in vitro* and *in vivo* optical imaging of a plethora of protein aggregates in cerebral amyloidoses. ACS Chem Biol;4:673–684.
112. Hammarstrom P., Simon R., Nystrom S., Konradsson P., Aslund A., Nilsson K.P. (2010) A fluorescent pentameric thiophene derivative detects *in vitro*-formed prefibrillar protein aggregates. Biochemistry;49:6838–6845.
113. Nilsson K.P., Aslund A., Berg I., Nystrom S., Konradsson P., Herland A., Inganas O., Stabo-Eeg F., Lindgren M., Westermark G.T., Lannfelt L., Nilsson L.N., Hammarstrom P. (2007) Imaging distinct conformational states of amyloid-beta fibrils in Alzheimer's disease using novel luminescent probes. ACS Chem Biol;2:553–560.
114. Nilsson K.P., Ikenberg K., Aslund A., Fransson S., Konradsson P., Rocken C., Moch H., Aguzzi A. (2010) Structural typing of systemic amyloidoses by luminescent-conjugated polymer spectroscopy. Am J Pathol;176:563–574.
115. Reinke A.A., Abulwerdi G.A., Gestwicki J.E. (2010) Quantifying prefibrillar amyloids *in vitro* by using a "thioflavin-like" spectroscopic method. Chembiochem;11:1889–1895.
116. Hu Y., Su B., Kim C.S., Hernandez M., Rostagno A., Ghiso J., Kim J.R. (2010) A strategy for designing a peptide probe for detection of beta-amyloid oligomers. Chembiochem;11:2409–2418.
117. Reinke A.A., Ung P.M., Quintero J.J., Carlson H.A., Gestwicki J.E. (2010) Chemical probes that selectively recognize the earliest abeta oligomers in complex mixtures. J Am Chem Soc;132:17655–17667.
118. Shi W., Dolai S., Rizk S., Hussain A., Tariq H., Averick S. *et al.* (2007) Synthesis of monofunctional curcumin derivatives, clicked curcumin dimer, and a PAMAM dendrimer curcumin conjugate for therapeutic applications. Org Lett;9:5461–5464.
119. Lenhart J.A., Ling X., Gandhi R., Guo T.L., Gerk P.M., Brunzell D.H., Zhang S. (2010) ''Clicked'' bivalent ligands containing curcumin and cholesterol as multifunctional abeta oligomerization inhibitors: design, synthesis, and biological characterization. J Med Chem;53:6198–6209.
120. Qin L., Vastl J., Gao J. (2010) Highly sensitive amyloid detection enabled by thioflavin T dimers. Mol Biosyst;6:1791–1795.
121. Chafekar S.M., Malda H., Merkx M., Meijer E.W., Viertl D., Lashuel H.A., Baas F., Scheper W. (2007) Branched KLVFF tetramers strongly potentiate inhibition of beta-amyloid aggregation. Chembiochem;8:1857–1864.